Role of Coupled Dynamics in the Catalytic Activity of Prokaryotic-like Prolyl-tRNA Synthetases

Brianne Sanford,[†,‡] Bach Cao,[†] James M. Johnson,[†] Kurt Zimmerman,[†] Alexander M. Strom,[†] Robyn M. Mueller,[†] Sudeep Bhattacharyya,*[,†] Karin Musier-Forsyth,*[,‡] and Sanchita Hati*[,†]

[†]Department of Chemistry, University of Wisconsin−Eau Claire, Eau Claire, Wisconsin 54702, United States
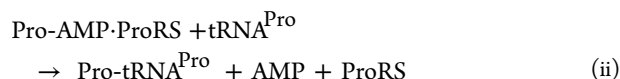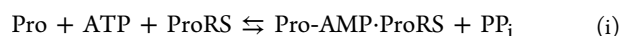[‡]Department of Chemistry and Biochemistry, Center for RNA Biology, The Ohio State University, Columbus, Ohio 43210, United States

Ⓢ Supporting Information

ABSTRACT: Prolyl-tRNA synthetases (ProRSs) have been shown to activate both cognate and some noncognate amino acids and attach them to specific tRNA^{Pro} substrates. For example, alanine, which is smaller than cognate proline, is misactivated by *Escherichia coli* ProRS. Mischarged Ala-tRNA^{Pro} is hydrolyzed by an editing domain (INS) that is distinct from the activation domain. It was previously shown that deletion of the INS greatly reduced cognate proline activation efficiency. In this study, experimental and computational approaches were used to test the hypothesis that deletion of the INS alters the internal protein dynamics leading to reduced catalytic function. Kinetic studies with two ProRS variants, G217A and E218A, revealed decreased amino acid activation efficiency. Molecular

dynamics studies showed motional coupling between the INS and protein segments containing the catalytically important proline-binding loop (PBL, residues 199−206). In particular, the complete deletion of INS, as well as mutation of G217 or E218 to alanine, exhibited significant effects on the motion of the PBL. The presence of coupled dynamics between neighboring protein segments was also observed through in silico mutations and essential dynamics analysis. Altogether, this study demonstrates that structural elements at the editing domain−activation domain interface participate in coupled motions that facilitate amino acid binding and catalysis by bacterial ProRSs, which may explain why truncated or defunct editing domains have been maintained in some systems, despite the lack of catalytic activity.
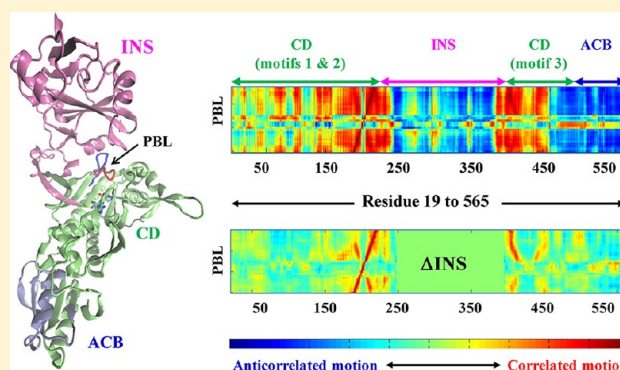
P rolyl-tRNA synthetases (ProRSs) are class II synthetases that catalyze covalent attachment of proline to the 3′-end of the tRNA^{Pro} in a two-step reaction:

$$Pro + ATP + ProRS \leftrightarrows Pro\text{-}AMP\cdot ProRS + PP_i \qquad (i)$$

$$Pro\text{-}AMP\cdot ProRS + tRNA^{Pro}$$
$$\rightarrow Pro\text{-}tRNA^{Pro} + AMP + ProRS \qquad (ii)$$

ProRSs from all three kingdoms of life are known to misactivate noncognate alanine and cysteine, resulting in mischarged tRNA^{Pro}.[1−3] To maintain high fidelity in protein synthesis, some ProRSs have acquired editing mechanisms to prevent misaminoacylation of tRNA^{Pro}.[1,2,4] On the basis of sequence alignments, ProRSs are classified into two broad groups: "eukaryotic-like" and "prokaryotic-like".[5,6] *Escherichia coli* (Ec) ProRS, a representative member of the prokaryotic-like group, is a multidomain protein. The catalytic domain (motifs 1−3, consisting of residues 64−81, 128−164, and 435−465, respectively) catalyzes the activation of proline and the aminoacylation of tRNA^{Pro}. The anticodon binding domain (residues 506−570) is critical for recognition of cognate tRNA. The insertion domain (INS; residues 224−407, located

between motifs 2 and 3 of the catalytic domain) is the post-transfer editing active site that hydrolyzes mischarged Ala-tRNA^{Pro}.[7,8] In contrast, Cys-tRNA^{Pro} is hydrolyzed by a free-standing editing domain known as YbaK present in some species.[9,10] Unlike prokaryotic-like ProRSs, eukaryotic-like ProRSs do not possess the INS but in some cases encode free-standing editing domain homologues.

In addition to post-transfer editing, the INS of Ec ProRS was found to have a significant impact on amino acid binding and activation.[11] Deletion of the INS (residues 232−394) of Ec ProRS resulted in a 200-fold increase in the K_M for proline. The overall proline activation efficiency was reduced by ~1200-fold relative to that of the wild-type (WT) enzyme.[11] Although the specific reason for this drastic effect is not understood, circular dichroism measurements demonstrated that deletion of the INS has no significant effect on the overall folding of the mutant protein.[11] Thus, it remains unclear what role the editing domain plays in substrate binding and amino acid activation.

It is known that for multidomain proteins like ProRS, coupled domain dynamics play an important role in catalytic function.[12,13] Although the relevance of the editing domain to amino acid activation by ProRS is not understood, a substrate-induced conformational change of a neighboring loop, known as the proline-binding loop (PBL, residues 199−206), was revealed by structural studies.[14] Three-dimensional structures of two bacterial ProRSs, *Rhodopseudomonas palustris* ProRS (Rp ProRS) and *Enterococcus faecalis* ProRS [Ef ProRS (Figure 1a)], showed an induced-fit binding mode with a large displacement (∼7 Å) of the PBL upon binding of the prolyl-adenylate analogue, 5′-O-[N-(prolyl)sulfamoyl] adenosine (Pro-AMS)
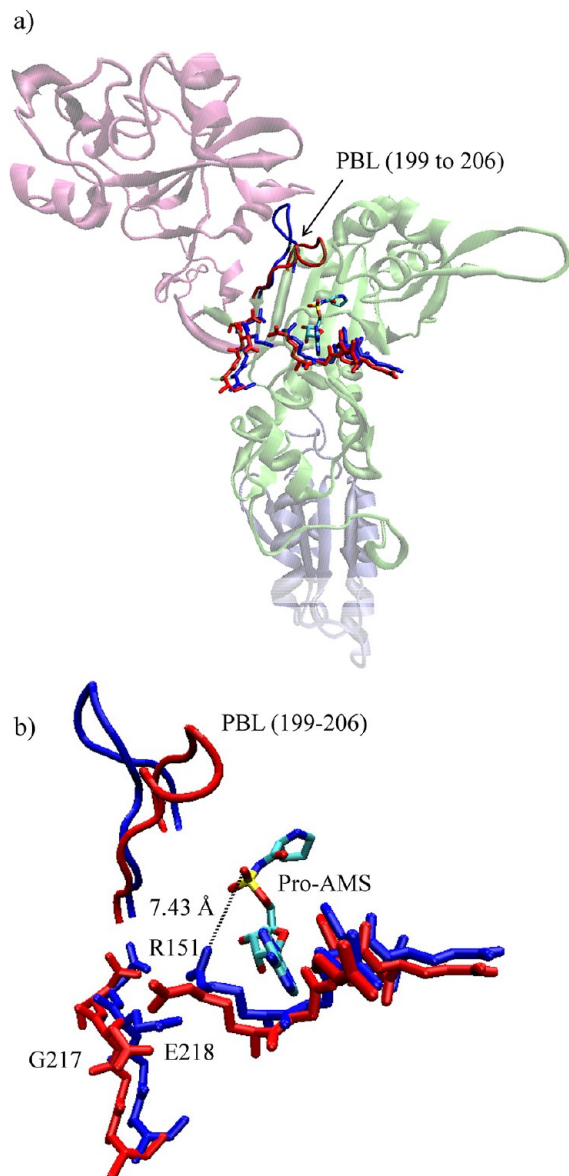

a)

PBL (199 to 206)

b)

PBL (199-206)

7.43 Å

Pro-AMS

R151

G217   E218

Figure 1. (a) Cartoon representation of the three-dimensional structure of the monomeric form of Ef ProRS (residues 1−570, PDB entry 2J3L, chain B). The structural domains are colored as follows: lime for the catalytic domain (residues 1−223 and 408−505), mauve for the editing domain (residues 224−407), and ice blue for the anticodon-binding domain (residues 506−570). The PBL is shown as tubes. G217, E218, R151, and the prolyl-adenylate analogue are shown as licorice: red for the "closed" state and blue for the "open" state. (b) Closer view of the PBL and the active site residues.

(Figure 1b).[14] Comparison of the substrate-bound and unbound structures also showed that the large displacement of the PBL was associated with the reorientation of several active site moieties, as well as some polypeptide segments that belong to the catalytic domain−editing domain interface.[14] These observations together with the observed dramatic change in Ec ProRS function upon deletion of the editing domain led us to hypothesize that the dynamics of structural elements proximal to the PBL influence substrate binding and catalysis by prokaryotic-like ProRSs.

To test the hypothesis described above, in this study the coupling of motions among various structural elements of Ec ProRS was investigated using computational and experimental approaches. In particular, to examine the effect of INS on the PBL dynamics, the motion of the full-length enzyme and the truncated enzyme (constructed by deletion of INS, hereafter termed ΔINS) was computationally simulated. Also, two highly conserved residues of the prokaryotic-like ProRS family, G217 and E218 (Figure 2), were mutated. These two residues,


```
EcoliProRS  AAYSKIFSRMGLDFRAVQALTGSIGGSASHEFQVLAQSGEDDVVFSDTSDYAANIELAEA 238
SenteProRS  AAYSRIFSRMGLDFRAVQALTGSIGGNASHEFQVLAQSGEDDIVFSDVSDYAANIELAEA 238
HinflProRS  QVYSNIFNRLGLDFRAVQALTGSIGGSASHEFQVLASSGEDDVVFSTESDFAANIELAEA 238
EfaecProRS  KAYTEVFKRCGLEFRSIIGDGGAMGGKDSKEFMAISEIGEDTICYSTESDYAANLEMATS 238
EfcalProRS  KAYSRIFERCGLEFRAIIGDGGAMGGKDSKEFMAISEIGEDTICYSTESDYAANLEMATS 238
LreutProRS  KAYRNIFDRIGLNYKVILALSGTMGGKNSQEFSAPAEVGEDIIAY-TDGDYAANIEKAES 238
BanthProRS  KAYSNIFARCGLNFRAVIALSGAMGGKDTHEFMVLSDVGEDTIAYSDTSDYAANIEMAPV 238
IpolyProRS  AAYTRIFERCGLKFRSVEADSGAIGGSGQEFHVLAESGEDEIIYCDSCGYAANLEKAES 238
CperfProRS  KAYVNIFNRCGLDAKAVAADSGAIGGSGSAEFMVKSEVGEDDVVFCTACDYAANIEKAPS 238
MtubeProRS  EAYQRIFDRLOVRYVIVSAVSGAMGGSASEEFLAESPSGEDAFVRCLESGYAANVEAVVT 240
```

PBL (199-206)   G217, E218

Figure 2. Portion of the multiple-sequence alignment of 10 prokaryotic-like ProRSs. The PBL and the highly conserved [217]GED[219] motif are boxed.

located at the junction of the activation domain and the editing domain, are not directly involved in catalysis but undergo substrate-induced conformational changes.[14] To evaluate the effect of mutation of these noncatalytic conserved residues on PBL dynamics and enzyme catalysis, enzyme motions were computationally simulated and kinetic parameters were determined experimentally. Taken together, the results of this study shed light on the role of distant domains and noncatalytic residues in producing a catalytically competent state for amino acid binding and activation by prokaryotic-like ProRSs.

■ MATERIALS AND METHODS

All experimental studies were performed using purified Ec ProRS. Because Ec and Ef ProRS possess a high degree of sequence identity (48%), computational studies were performed starting with the X-ray crystallographic structure of Ef ProRS [PDB entry 2J3M ("open" state)],[14] and the results were compared with results using a homology model of Ec ProRS developed using Ef ProRS as a template (provided by S. Cusack). All simulations were performed with apoenzymes.

■ EXPERIMENTAL METHODS

Materials. All amino acids (Sigma) were of the highest quality (>99% pure) and used without further purification. Tritiated proline (83 Ci/mmol) and alanine (75 Ci/mmol) were from Perkin-Elmer. Primers for site-directed mutagenesis and polymerase chain reaction were from Integrated DNA Technologies.

Enzyme Preparation. Overexpression and purification of histidine-tagged[4] WT and mutant Ec ProRS were performed as

described previously.[15,16] Plasmids encoding G217A and E218A Ec ProRS were generated by QuikChange mutagenesis (Stratagene) of pCS-M1S[16] using the following primers: G217A, 5′-GCG CAG AGC **GCG** GAA GAC GAT GTG G-3′ (top) and 5′-CCA CAT CGT CTT CCG CGC TCT GCG C-3′ (bottom); E218A, 5′-GCG CAG AGC GGT **GCG** GAC GAT GTG G-3′ (top) and 5′-CAA CAT CGT CCG CAC CGC TCT GCG C-3′ (bottom). Results of mutagenesis were confirmed by DNA sequencing (University of Wisconsin, Biotechnology Center, Madison, WI). Protein expression was induced in Ec SG13009 (pREP4) competent cells with 1 mM isopropyl β-D-thiogalactoside for 4 h at 37 °C. Histidine-tagged proteins were purified using a Talon cobalt affinity resin, and the desired protein was eluted with 100 mM imidazole. Protein concentrations were determined initially by the Bio-Rad Protein Assay (Bio-Rad Laboratories) followed by active site titration.[17]

RNA Preparation. Ec tRNA^{Pro} was transcribed using T7 RNA polymerase from the BstN1-linearized plasmid as described previously[18] and purified by denaturing 12% polyacrylamide gel electrophoresis.

ATP–PP$_i$ Exchange Assays. The ATP–PP$_i$ exchange assay was performed at 37 °C according to the published method.[19] The concentrations of proline and alanine ranged from 0.025 to 50 mM and from 1 to 850 mM, respectively. The enzyme concentrations used were 10−20 nM for proline and 250−500 nM for alanine activation. Kinetic parameters were determined from Lineweaver−Burk plots and represent the average of at least three determinations.

ATP Hydrolysis Assays. ATP hydrolysis reactions for monitoring pretransfer editing were conducted as described previously.[11] An alanine concentration of 500 mM was used and a proline concentration of 30 mM. The reactions were initiated with a final ProRS concentration of 0.5 μM.

Aminoacylation Assays. Aminoacylation assays were performed under standard conditions[20] with 0.5 μM tRNA^{Pro}, 13.3 μM [^{3}H]proline, and 100 nM ProRS.

Aminoacylated tRNA. Aminoacylated tRNA for use in deacylation assays was prepared at room temperature according to published conditions.[1] Ec AlaRS (2 μM) was used to acylate G1:C72/U70 tRNA^{Pro} (8 μM) in the presence of [^{3}H]Ala (7.3 μM) in buffer containing 50 mM HEPES (pH 7.5), 4 mM ATP, 25 mM MgCl$_2$, 20 mM β-mercaptoethanol, 20 mM KCl, and 0.1 mg/mL bovine serum albumin.

Deacylation Assays. Deacylation assays were conducted at room temperature according to published conditions.[1] Reaction mixtures contained 1 μM G1:C72/U70 [^{3}H]Ala-tRNA^{Pro}, 150 mM KPO$_4$ (pH 7.0), 5 mM MgCl$_2$, and 0.1 mg/mL bovine serum albumin. The reactions were initiated with 5 μM ProRS. Negative controls were performed using 150 mM KPO$_4$ (pH 7.0) in place of ProRS.

■ COMPUTATIONAL METHODS

Molecular Dynamics Simulations. MD simulations were conducted starting with the crystallographic structure of Ef ProRS [chain B, PDB entry 2J3M (open, residues 19−565)]. The ΔINS (constructed by replacing INS residues 232−394 with a 16-residue Gly$_{12}$Ser$_4$ linker[11]) and the three mutants (G217A, E218A, and E218D) were generated with the Mutator plug-in of Visual Molecular Dynamics (VMD) version 1.8.6.[21] For all simulations, the all-atom CHARMM22 force field[22] was used within the NAMD[23] package. The three-point charge TIP3P model[24] was used to represent solvent water. Non-

bonded interactions were truncated using a switching function between 10 and 12 Å, and the dielectric constant was set to unity. The SHAKE algorithm[25] was used to constrain bond lengths and bond angles of water molecules and bonds involving a hydrogen atom. The MD simulations were performed using isothermal−isobaric (NPT) conditions. Periodic boundary conditions and particle mesh Ewald methods[26] were used to account for the long-range electrostatic interactions. In all MD simulations, a time step of 2 fs was used. The pressure of the system was controlled by the implementation of the Berendsen pressure bath coupling[27] as the temperature of the system was slowly increased from 100 to 300 K. During the simulations at 300 K, the pressure was kept constant by applying the Langevin piston method.[28,29]

The WT and mutant proteins were solvated with water in a periodic rectangular box with dimensions of 130 Å × 78 Å × 92 Å with water padding of 12 Å between the walls of the box and the nearest protein atom. The charge neutralization (with sodium ions) of the solvated system was performed with the VMD autoionize extension.[21] The resultant systems, containing ∼84000 atoms (∼74000 atoms for ΔINS ProRS), including approximately 16450 water molecules and 33 sodium ions (32 and 14 ions for E218A and ΔINS ProRS, respectively), were equilibrated by slightly modifying previously described procedures.[30,31] Briefly, solvated proteins were further subjected to 1000 steps of conjugate gradient minimization at 100 K. The temperature of the solvated systems was then increased to 300 K in 3000 steps and was further equilibrated at 300 K for 500 ps. The equilibrated system was then used in 12 ns simulations. The equilibration and stability of the dynamics were checked by calculating the root-mean-square deviations (RMSDs) of C$_\alpha$ atoms from their initial coordinates.

Essential Dynamics. The collective dynamics of the protein was studied through essential dynamic analysis,[32−34] which involves computation of the principal components of atomic fluctuations. The last 7 ns of the 12 ns MD simulation data was used to extract the principal modes of collective dynamics (called principal components) using Carma.[35] The mathematical operation behind essential dynamics is called principal component analysis (PCA), which takes a data set from a trajectory of a long time-scale MD simulation as input and extracts the low-frequency (high-amplitude) collective motions of the biomolecule, which are often more relevant for its functions.[36] The principal components were computed by performing eigenvalue decomposition of a covariance matrix, and the mathematical formalism is described elsewhere.[37] Briefly, the covariance matrix, **C** is computed with elements C_{ij} for any two points (C$_\alpha$ coordinates) i and j using

$$C_{ij} = \langle (x_i - \langle x_i \rangle)(x_j - \langle x_j \rangle) \rangle \tag{1}$$

where x_1, x_2, ..., and x_{3N} are the mass-weighted Cartesian coordinates of an N-particle system and the angular brackets represent an ensemble average calculated over all sampled structures from the simulations. Next, the symmetric $3N \times 3N$ matrix **C** can be diagonalized with an orthonormal transformation matrix **R**

$$\mathbf{R^T C R} = \text{diag}(c_1, c_2, ..., c_{3N}) \tag{2}$$

where c_1, c_2, ..., and c_{3N} are eigenvalues; columns in transformation matrix **R** are eigenvectors, which are also called the principal modes. If $X(t)$ represents the time-evolved

Table 1. Kinetic Parameters for Amino Acid Activation by WT, E218A, and G217A Ec ProRS[a]

	amino acid	k_{cat} (s^{-1})	K_M (mM)	k_{cat}/K_M (s^{-1} mM^{-1})	relative k_{cat}/K_M	fold change
WT	proline	12.7 ± 4.9	0.228 ± 0.028	55.7	1	−
	alanine	3.52 ± 2.1	685 ± 360	0.00513	1	−
E218A	proline	4.4 ± 2.2	3.40 ± 0.68	1.29	0.0232	43
	alanine	3.26 ± 5.4	1360 ± 1300	0.0024	0.468	2
G217A	proline	3.37 ± 1.1	0.427 ± 0.077	7.89	0.142	7
	alanine	2.18 ± 0.23	454 ± 78	0.0048	0.935	0

[a]Results are the average of three trials with the standard deviation indicated. In each, the k_{cat}/K_M of the mutant is relative to the WT kinetics with the corresponding amino acid.

coordinates (trajectory) of the water-encapsulated protein active site, it can be projected onto the eigenvectors

$$q = \mathbf{R^T}[X(t) - \langle X \rangle] \qquad (3)$$

The projection is a measure of the extent to which each conformation is displaced, in the direction of a specific principal mode, and is called the principal component (PC). For a trajectory, the projections are obtained as matrix elements $q_i(t)$ (i = 1, 2, ..., M).

PCA was conducted using the following steps: (i) preparing a modified trajectory file by removing the coordinates of the water molecules, selecting only the C_α atoms, and removing the overall translational and rotational motions, (ii) calculating the covariance matrix in which the atomic coordinates are the variables, and (iii) diagonalizing the covariance matrix for calculation of the eigenvectors and the corresponding eigenvalues. The first three PCs were used for performing PCA-based cluster analysis as discussed in Carma documentation.[35] Briefly, on the basis of contributions of the first three PCs, conformations in the overall trajectory were grouped into several clusters. The cluster with the greatest number of conformations is representative of predominant conformational fluctuations and was used for further analysis of dynamic cross-correlations between C_α atoms. The cross-correlation coefficient between fluctuations of residues i and j (CC_{ij}) was calculated using

$$CC_{ij} = \frac{\langle (x_i - \langle x_i \rangle)(x_j - \langle x_j \rangle) \rangle}{\sigma_{x_i} \sigma_{x_j}} \qquad (4)$$

where σ_{x_i} and σ_{x_j} represent the standard deviation of the displacements of the two points (C_α coordinates) i and j, respectively. The correlated motion ($CC_{ij} > 0$) between two C_α atoms occurs when they move in the same direction, while the anticorrelated motion is generated when two C_α ($CC_{ij} < 0$) atoms move in opposite directions.

The root-mean-square projections (RMSP) of q were obtained from the last 7 ns of the simulations using the following equation:

$$RMSP = \sqrt{\frac{1}{M} \sum_{i=1}^{conf} [q_i(t)]^2} \qquad (5)$$

To determine if the functional dynamics had undergone significant change because of a single-point mutation, a combined essential dynamics analysis was performed following literature methods.[32−34] In this procedure, a comparison of dynamics of five protein systems was conducted by concatenating their trajectories to produce a combined covariance matrix. The separate trajectories were then projected

onto the resulting eigenvectors, and the properties of these projections were compared for these simulations.

◼ RESULTS

The results are presented in the following order. First, the experimental results are reported to show the impact of mutation of the two strongly conserved noncatalytic residues on the enzyme function. Next, the results of the MD simulations are presented to illustrate the flexibility of the ProRS and the overall coupling of various structural elements surrounding its catalytic site. Finally, the molecular-level impact of mutations (deletion and site-directed mutations) on the catalytically important PBL dynamics was characterized through essential dynamics analysis.

Activation of Proline and Alanine. To investigate the role of the $^{217}GED^{219}$ motif in maintaining coupled motions among the protein segments surrounding the synthetic active site, the effect of mutation of G217 and E218 on the function of the enzyme was experimentally tested. The kinetic parameters for proline and alanine activation were determined for both mutants and compared with those of WT Ec ProRS. We found that E218A ProRS activates proline but with a decreased k_{cat} (3-fold) and an elevated K_M [15-fold (Table 1)]. Overall, the proline activation efficiency of this mutant was decreased 45-fold compared to that of the WT enzyme. Reduced catalytic efficiency for proline activation was also observed for the G217A mutant. The k_{cat}/K_M of G217A ProRS was reduced 7-fold relative to that of the WT enzyme (Table 1). In contrast, alanine activation by the G217A mutant was not affected compared to that of the WT enzyme, and an only 2-fold decrease in the extent of alanine activation was observed for the E218A mutant (Table 1).

Aminoacylation of tRNA^{Pro}. The effect of mutation of G217 and E218 on aminoacylation of proline was also tested. Both G217A and E218A can charge proline onto tRNA^{Pro}, albeit with 3-fold reduced efficiency (Figure 3a).

Pretransfer Editing. Stimulation of ATP hydrolysis is considered indicative of pretransfer editing, presumably because the noncognate amino acids that are hydrolytically edited are repeatedly reactivated by the synthetase, consuming ATP in each cycle.[38] In contrast, the cognate amino acid is bound to the synthetase until it is transferred to the tRNA. Ec ProRS possesses tRNA-independent pretransfer editing against alanine.[39] Here, we tested the pretransfer editing activity of the two mutant proteins and compared them with the WT activity. ATP hydrolysis was stimulated in the presence of alanine for both mutants. However, E218A ProRS exhibited reduced activity (9-fold) compared to that of the G217A variant, which possessed editing activity that was comparable to that of the WT enzyme (Figure 3b). The reduced activity of
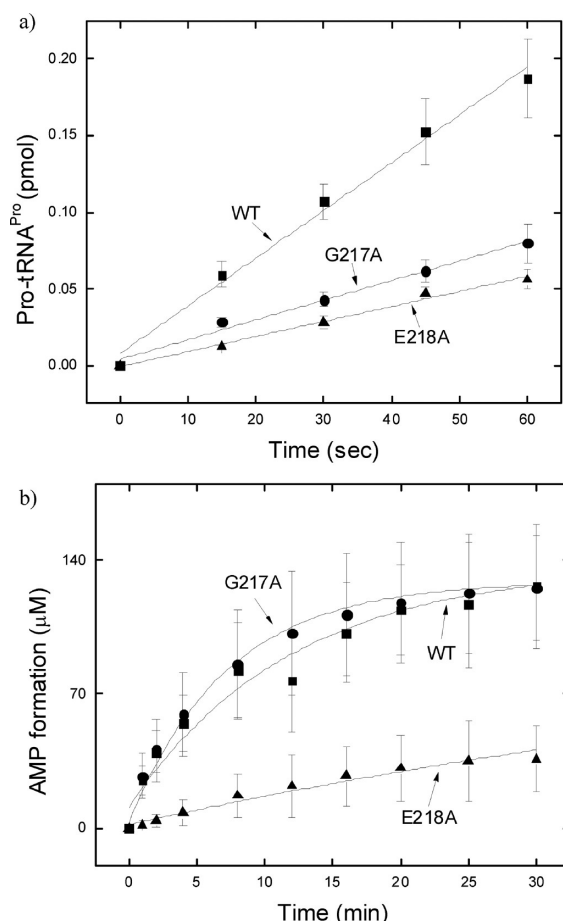
Figure 3. (a) Aminoacylation of tRNA^{Pro} with proline by WT, G217A, and E218A Ec ProRS. The assay was performed at 37 °C with 0.5 μM tRNA^{Pro} and 100 nM Ec ProRS. (b) Pretransfer editing in the presence of alanine by WT, G217A, and E218A Ec ProRS. The assay was performed at 37 °C using 0.5 μM ProRS and 500 mM alanine. Lines are single-exponential fits of the data.

E218A ProRS may, in part, be due to its poor alanine activation efficiency.

Post-Transfer Editing. The post-transfer editing activity of WT and variant ProRSs was also tested by monitoring the hydrolysis of misacylated Ala-tRNA^{Pro}. All three enzymes exhibited similar post-transfer editing activity (Figure S1 of the Supporting Information). Thus, the binding of the mischarged tRNA in the editing active site and the hydrolysis of the ester bond were not affected by mutations at the editing domain−activation domain interface.

Root-Mean-Square Deviation (RMSD) Profiles. The RMSDs were calculated using 12 ns MD simulation data for WT, G217A, E218A, E218D, and ΔINS ProRS systems. The plots of RMSD with respect to the initial equilibrated structure are shown in Figure 4. After ∼5 ns simulations, the C$_\alpha$ RMSD values remained within ∼1 Å. Data from the last 7 ns simulations were used for further study.

Flexible Regions. B factor analysis revealed several highly flexible regions in Ef ProRS. A plot of normalized experimental B factors (crystallography[14]) and calculated B factors (using Carma[35]) of the C$_\alpha$ atoms of WT Ef ProRS is shown in Figure 5. The flexible regions identified by both experimental and computational methods are comparable, except for residues 75−125 and the PBL. It appears that the flexibility of these two
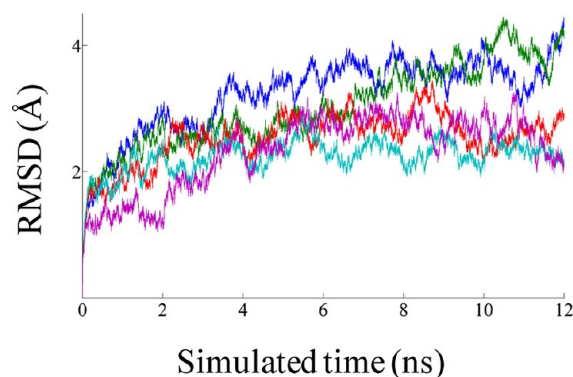

Figure 4. RMSDs of the C$_\alpha$ atoms from their initial coordinate as a function of time. Calculations of RMSDs for WT (blue), G217A (green), E218A (red), E218D (cyan), and ΔINS (purple) Ef ProRS were performed using 12 ns MD simulation data.
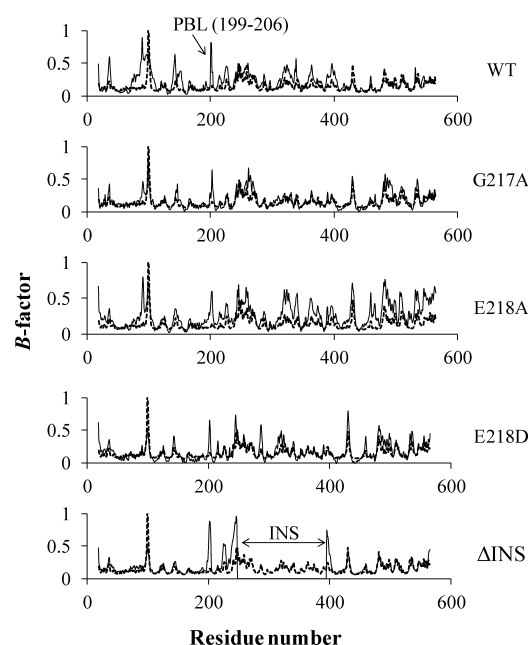

Figure 5. Comparison of the normalized C$_\alpha$ B factors obtained from the crystal structure (gray dotted line; PDB entry 2J3M, chain B) and calculated from MD simulation data (black solid line). For ΔINS, the calculated B factors are missing for residues 232−394.

regions is experimentally underestimated, possibly because of the crystal packing arrangement of the protein.

In the case of the two mutants obtained by conservative mutation, G217A and E218D, the overall protein flexibility was reduced compared to that of the WT enzyme (Figure 5). However, the substitution of E218 with alanine resulted in the increased flexibility of the protein backbone, especially for the C$_\alpha$ atoms of the INS and C-terminal domain. Interestingly, in all three mutants (G217A, E218A, and E218D), the flexibility of the PBL was reduced compared to that of the WT protein. On the other hand, the complete deletion of the INS resulted in a less flexible protein with B factors almost comparable to the experimentally observed results except for the PBL, which becomes more flexible in the absence of the INS (Figure 5).

Dynamic Cross Correlations and Essential Dynamics Analyses. The dynamic cross-correlation map obtained from the MD simulation of Ef ProRS (chain B) is shown in Figure 6. In this study, the dynamic cross-correlation matrix was
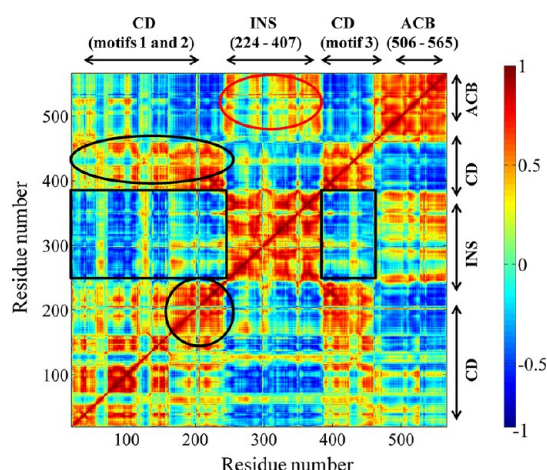
Figure 6. Dynamic cross-correlations between the C_α atoms of Ef ProRS obtained from the cluster analysis and PCA. A value of +1.0 was set for strongly correlated motion (red), whereas −1.0 was used for strongly anticorrelated motions (blue). The boxed and circled regions are discussed in the text. Abbreviations: CD, catalytic domain; INS, insertion domain; ACB, anticodon binding domain.

Figure 7. Dynamic cross-correlations between the C_α atoms of the PBL-containing protein segment (residues 190−220) vs C_α atoms of residues 19−565 of the WT and mutant ProRSs. Color coding is as described in the legend of Figure 6. For ΔINS, the region for the cross-correlations between residues 190−220 and INS residues 247−394 is shown in a green rectangle. Residues 232−394 are replaced with a 16-residue linker in this plot.

generated using the first three PCs. Analysis of the cross-correlation of fluctuations of residues for the first three PCs revealed both inter- and intradomain motional correlation. It was found that the activation domain and the INS are mainly engaged in anticorrelated motions; i.e., their displacements are in opposite directions [$CC_{ij} < 0$ (Figure 6, black rectangles)]. An anticorrelated pattern of motions was also observed between the catalytic domain residues and the anticodon binding elements of Ef ProRS. On the other hand, the motion of the editing domain and the anticodon binding domain is weakly correlated [$CC_{ij} > 0$ (Figure 6, red oval)].

Various structural elements within the catalytic domain, which are essential for substrate binding and catalysis, are engaged in correlated motions (Figure 6, black oval). As expected, the adjacent residues of the protein segment (residues 190−220) containing the PBL and the [217]GED[219] motif are engaged in strong correlated motion (Figure 6, black circle). Also, the motion of the PBL-containing protein segment is mostly correlated in nature with respect to motifs 1−3 of the catalytic domain. However, its motion is anticorrelated with respect to the INS and the anticodon binding domain.

The effects of deletion of INS as well as point mutations of G217 and E218 on Ef ProRS dynamics were also studied. The dynamic cross-correlation map of the atomic (C_α) fluctuations between the PBL-containing protein segments (residues 190−220) and the rest of the molecule for the WT and the mutant variants is shown in Figure 7. Although we cannot rule out the change in structure due to these mutations (site-directed/deletion), noticeable alteration of residue fluctuations between the PBL-containing protein segment and other structural elements of the protein was observed for all mutant proteins compared to the WT enzyme (Figure 7). In particular, a significant change in the motional coupling between the PBL-containing segment and the editing domain (residues 224−407) was observed for the two ProRS variants, G217A and E218D. In addition, noticeable alteration of dynamic coupling among residues of the entire PBL-containing segment (residues 190−235) and residues 150−235 as well as anticodon binding domain was observed (Figure 7).
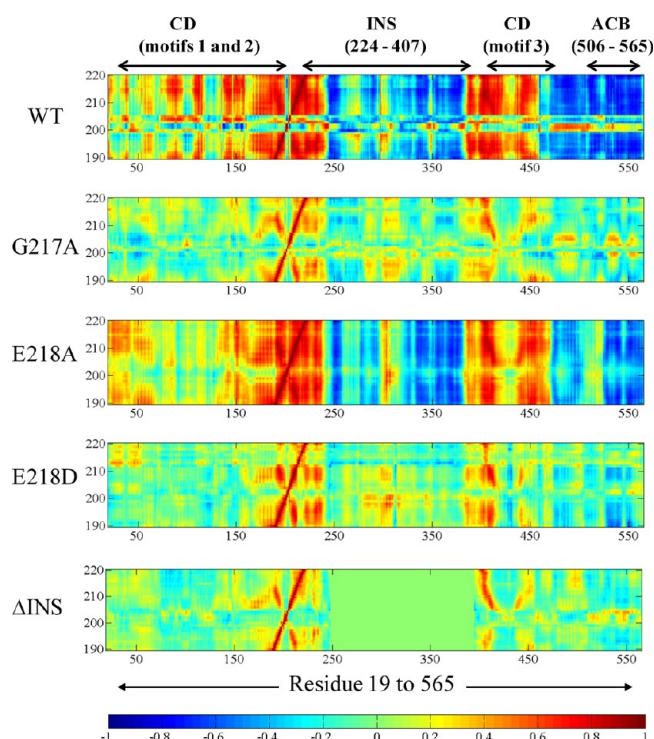
Combined Essential Dynamics. To examine the impact of the deletion of INS or point mutation in the [217]GED[219] motif on the collective dynamics of the PBL, we analyzed the essential dynamics of WT Ef ProRS and mutant variants using the last 7 ns of the 12 ns MD simulation data. Specifically, we performed a "combined" essential dynamics analysis,[32,33] using the concatenated trajectories (of the C_α atoms) of all five proteins (WT, ΔINS, G217A, E218A, and E218D).

The combined essential dynamics analysis clearly shows that each mutation has an impact on the collective PBL (residues 190−210) dynamics. The RMSP's (eq 5) as a function of eigenvector indices for the WT and mutant proteins of Ef ProRS are shown in Figure 8. The fluctuation of the PBL along PC1 is significantly altered for all the mutant proteins compared to that of the WT enzyme. Noticeable changes were also observed for PC2 and PC3. Therefore, this analysis indicates that the deletion of the INS or mutation at the junction of the INS and activation domain could impact PBL dynamics and potentially alter substrate binding. Similar differences in the slow dynamics of the PBL upon mutation of G217 and E218 to alanine were observed for Ec ProRS (Figure S2 of the Supporting Information).

The alteration of the dynamics of the PBL either due to the deletion of the INS or due to mutations in the [217]GED[219] motif can be visualized from the superimposition of conformations of the PBL extracted from the essential dynamics analysis. These superimposed conformations correspond to the dynamics of the PBL along the three PCs (i.e., in the direction of collective dynamics) and are displayed in Figure 9. Only backbone C_α atoms are shown for the sake of clarity. In the C_α traces, it is
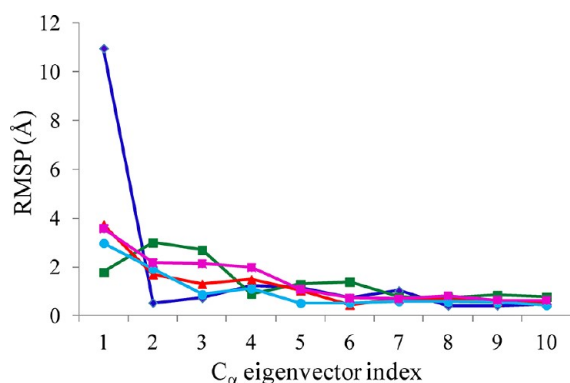
Figure 8. Combined analysis of the computed root-mean-square projections (RMSP, eq 5) over the last 7 ns of 12 ns simulation data for eigenvectors 1−10 for WT (blue), G217A (green), E218A (red), E218D (cyan), and ΔINS (purple) Ef ProRS.
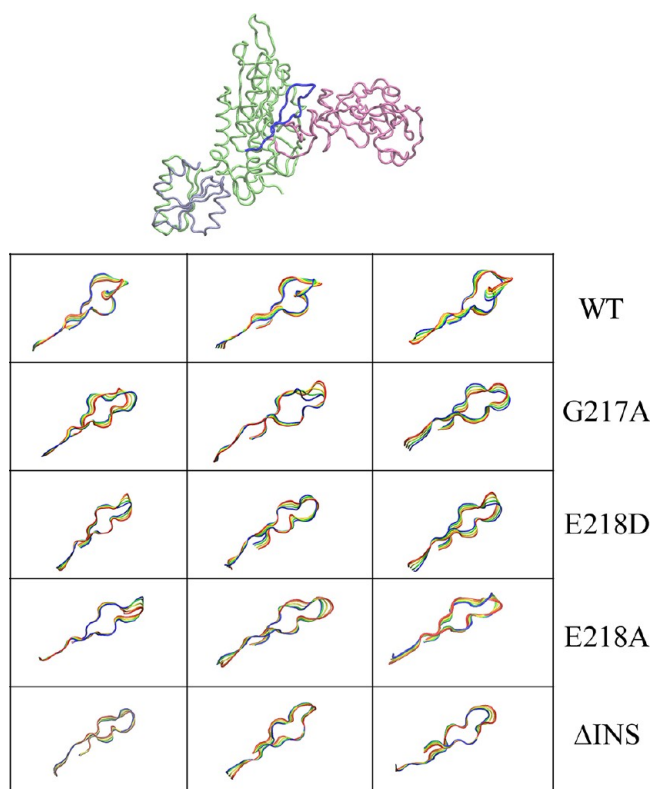

Figure 9. Visual representation of the movement of the PBL. Superposition of four configurations extracted from the concatenated trajectories by projecting the C_α motion onto eigenvectors 1−3. The four conformations are colored blue (starting), green, yellow, and red (end).

apparent that the pattern of the collective dynamics of the PBL (along the first three PCs) was altered by the point mutation at the domain−domain interface as well as by the deletion of the INS. Taken together, combined essential dynamics analysis revealed that deletion of INS or point mutations at the catalytic domain−editing domain junction caused perceptible changes in the collective PBL dynamics.

■ DISCUSSION

Protein Dynamics and Catalysis. Dynamics is an intrinsic property, encrypted in the three-dimensional structure and folding of a protein. Collective dynamics are prevalent in modular proteins and play an important role in enzyme function. In fact, simulations of mechanochemical properties of enzymes have shown that coupling between catalytic function and collective dynamics is a prerequisite for enzyme activity.[40] Several other studies have also revealed that internal motions essentially represent the intrinsic mechanical properties of an enzyme and do not originate from the presence of a substrate. Nevertheless, these internal protein motions facilitate substrate recognition and binding and thereby promote catalysis.[41−43] In addition, studies have demonstrated that protein motions can modify the catalytic rate by influencing the height of the activation free energy barrier and the transmission coefficient (i.e., the capacity of recrossing the barrier).[44−46] For example, a direct correlation between the frequencies of enzyme motions and catalytic turnover rates was observed in cyclophilin A using NMR relaxation experiments.[46]

A number of studies indicate that internal protein motions involve networks of residues extending beyond the catalytic site.[41,44,45] Enzyme catalysis is found to be augmented by coupled motion through these networks amidst growing evidence that the slower collective protein motions and the faster bond-breaking or -forming motions are connected. An example of such a synergistic relationship can be found in adenylate kinase,[47] where faster (pico- to nanosecond time scale) atomic fluctuations at the hinge regions were found to promote the large-scale displacement of the lid during substrate binding. Also, studies of several enzymes, including dihydrofolate reductase and liver alcohol dehydrogenase,[42,45,48] have demonstrated that mutations of noncatalytic residues alter their catalytic function by modifying internal enzyme motions. Taken together, there is an overwhelming amount of evidence showing the significance of coupled dynamics in enzyme function. The role of coupled dynamics in the structure and function of ProRS has remained unexplored and constitutes the basis of this investigation.

Proposed Role of the Editing Domain. To probe the hypothesis that the collective dynamics involving the editing domain regulate substrate binding and catalysis by ProRS, the motion of ΔINS construct was compared with that of the full-length WT enzyme. In addition, two noncatalytic but conserved residues (G217 and E218) in the editing domain−activation domain junction were chosen for mutagenesis. If coupled internal dynamics truly exists between structural elements in the vicinity of the PBL, then point mutations in any of these elements should alter the dynamics, as well as the efficiency, of catalysis.

Amino Acid Activation and Aminoacylation. Experimental studies show that G217 and E218 are critical for enzyme catalysis. The X-ray crystal structure of bacterial ProRS shows strong interactions between E218 and a conserved arginine residue [R151 of Ef ProRS (see Figure 1b)] that helps to stabilize the phosphate group of the substrate ATP molecule.[14] Indeed, a 45-fold decrease in the level of proline activation was measured in the case of E218A ProRS, showing that this residue is critical for cognate amino acid activation. However, only a small decrease (∼2-fold) in alanine activation efficiency was observed for this mutant. A 7-fold decrease in proline activation efficiency upon mutation of G217 to alanine was observed, although this residue does not interact directly with any catalytic site residues. The lack of a significant effect on alanine activation for the E218A and G217A variants suggests that these residues might aid in maintaining the

internal dynamics of the active site protein segments and the PBL, which facilitates the binding of the cognate amino acid but plays a more minor role in noncognate alanine activation. This is also apparent from the fact that the k_{cat} for proline activation by E218A ProRS was only reduced 3-fold, whereas the K_M was elevated 15-fold.

The mutation of G217 and E218 to alanine also impacted cognate tRNA aminoacylation (Figure 3a), although the impact was less severe (~2−3-fold) than for amino acid activation. This observation suggests that the binding of the 3′-acceptor end in the aminoacylation active site was not altered significantly by the alanine substitutions.

Role of PBL in Amino Acid Selection. If the open to closed conformational transition of the PBL is important for the protection of the cognate aminoacyl adenylate from spontaneous hydrolysis by the surrounding water, the mutation of G217 and E218 to alanine may be expected to enhance Pro-AMP hydrolysis. However, ATP hydrolysis was only slightly stimulated in the presence of proline for the G217A and E218A mutants (Figure S1a of the Supporting Information), suggesting that the main role of the PBL is to facilitate amino acid selection and binding. Moreover, no noticeable difference in post-transfer editing activity was observed for these mutants relative to that of the WT enzyme (Figure S1b of the Supporting Information), demonstrating that mutations in the ^{217}GED^{219} motif do not affect binding and hydrolysis of misacylated tRNA^{Pro}.

Flexibility and Collective Protein Dynamics. The *B* factor calculations performed on the Ef ProRS demonstrated that the PBL is quite flexible (Figure 5). However, the flexibility of this loop was altered by the mutation of G217 and E218. As expected, mutation of G217 to alanine brought some rigidity to the PBL dynamics. On the other hand, mutation of E218 to alanine caused an increase in the mobility of the whole protein backbone but reduced the flexibility of the PBL. The increased mobility of the protein backbone is expected as the substitution of E218 with alanine disrupted the electrostatic interaction between E218 and R151 of the activation domain (Figure 1b). Interestingly, the mutation of E218 to aspartic acid resulted in an overall reduction in protein flexibility. Close scrutiny of the E218D structure revealed the existence of some additional H-bond interactions between the surrounding residues and the aspartic acid, which might have brought some extra rigidity to the structure (data not shown). However, the deletion of the INS has the reverse effect on the flexibility of the PBL. Apparently, the PBL that is essential for substrate binding and catalysis acquired significant flexibility upon deletion of the INS (Figure 5). This observation suggests that the INS might have a role in maintaining the optimal flexibility of the PBL.

The cross-correlation matrix obtained from the cluster analysis (eq 4) revealed that the editing domain is mainly engaged in anticorrelated motion with the central activation domain (Figure 6). The existence of anticorrelated motion between these two domains may be critical for providing adequate space for the 3′-end of a tRNA to enter the synthetic active site for aminoacylation. Anticorrelated motion between the editing and activation domains has also been observed in other synthetase systems, including isoleucyl- and leucyl-tRNA synthetases.[49,50] Close analysis of the dynamic cross-correlation matrix also revealed the existence of correlated motion among several polypeptide segments within the activation domain. In addition, the adjacent residues of the polypeptide segment that includes both the PBL and the ^{217}GED^{219} motif (residues 195−

225) are found to be engaged in correlated motion among themselves and anticorrelated motion with most of the editing domain elements. Moreover, the simulated collective dynamics analysis of the WT versus mutant ProRSs revealed that mutation of noncatalytic residues and deletion of INS indeed alter the dynamics of the PBL with respect to the rest of the protein. Analysis of the dynamic cross-correlations between the PBL and other amino acid residues of Ef ProRS (Figure 7) demonstrated that the extent of correlation or anticorrelation between residue fluctuations depends upon neighboring as well as distant residues. It also showed that the anticorrelated motion between the editing domain and PBL undergoes a perceptible change in the case of the G217A, E218A, and E218D variants.

The effect of alanine substitutions at G217 and E218 on the PBL dynamics was also evident from the combined essential dynamics analysis, which showed significant changes in the RMSP of the first three major modes (eigenvectors) of collective dynamics of the PBL (Figure 8). Interestingly, the combined PC analysis shows the deletion of INS or mutation of G217 and E218 has a comparable effect on the collective PBL dynamics (Figures 8 and 9). Although these simulations were conducted in the absence of substrate, the analysis suggests that mutation of residues so close to the PBL has an impact on the movement of the PBL as significant as that observed for the deletion of the whole INS. Taken together, these observations suggest that coupled dynamics are relevant for PBL movement and, therefore, could impact substrate binding and catalysis.

Examination of the polypeptide segment (residues 190−220) at the interface of the activation and editing domains reveals the presence of a number of negatively charged residues, namely, E209, E218, D219, E234, and E407 (Figure 10). These residues, which are conserved in both Ef and Ec ProRSs, are
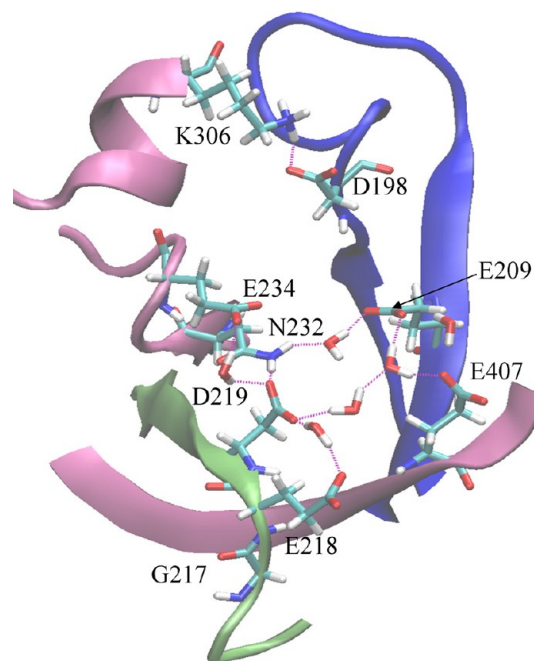

Figure 10. View of the region of Ef ProRS (PDB entry 2J3M, chain B) adjacent to the PBL and the "GED" motif showing charged residues at the activation domain−editing domain interface. The color coding is as follows: mauve for editing domain elements, blue for the PBL, and lime for the GED motif.

hydrogen-bonded to each other through water molecules and other polar residues like N232 and display significant correlations in the direction of their motions (Table 2).

Table 2. Correlation Coefficients (CC_{ij}, eq 4) of Fluctuations of Residue Pairs in Ef ProRS, Which Were Observed To Be Engaged in Hydrogen Bonding (Figure 10)

amino acid pair	CC_{ij}			
	WT	G217A	E218A	E218D
D219···E209	0.70	0.35	0.70	0.34
E218···E209	0.58	0.30	0.75	0.24
D219···N232	0.54	0.42	0.71	0.40
E209···N232	0.79	0.44	0.80	0.66
E209···E234	0.65	0.12	0.69	0.55
D219···E407	0.77	0.48	0.74	0.35
E218···E407	0.81	0.45	0.78	0.28
M202···T241	0.72	−0.01	0.09	0.03
G203···T241	0.73	0.13	0.01	−0.08
G203···D347	0.63	0.11	−0.09	0.10
M202···E352	0.62	−0.17	−0.10	−0.03
M202···S380	0.69	−0.10	−0.08	0.28
G203···E382	0.64	0.15	0.01	0.10
G203···D383	0.61	0.07	0.39	0.22
M202···E382	0.50	0.14	0.26	0.00
M202···D383	0.60	0.01	0.21	0.23

Interestingly, the dynamic correlations among these residues of the INS and the extended part of the PBL were maintained in the E218A variant, whereas correlations between these polar residues were significantly reduced in the case of G218A and E218D mutants (Table 2). On the other hand, analysis of the dynamic coupling between the tip of the PBL (M202 and G203) and several surrounding structural elements (residues 239−244, 345−351, and 378−383) of the INS (not shown) revealed that the movements of these editing domain segments are significantly correlated to the tip of the PBL in the WT enzyme. However, these distant correlations are completely abolished in all three mutants (Table 2). These observations suggest that mutation of either G217 or E218 has a strong impact on the collective motion of the PBL despite their varied local impacts. Moreover, structural analysis of the WT and mutant enzymes revealed that INS protein segments are approximately 2−3 Å closer to the tip of the PBL (residues 201−204) in the WT enzyme than in the mutant proteins. These neighboring structural elements appear to be critical for maintaining the coupled dynamics between the two functional domains, as well as the optimal flexibility of the PBL. Therefore, the observed dramatic effect on enzyme catalysis in the INS deletion mutant[11] is fully consistent with our results.

■ CONCLUSIONS

The combined use of computer simulations and mutational analysis has allowed a better understanding of the role of domain dynamics in the enzymatic function of prokaryotic-like ProRSs (Figure 1). Experimental mutational studies of two conserved residues, G217 and E218 (Figure 2), revealed significantly reduced catalytic efficiency, while essential dynamics analysis of these mutant proteins showed a reduction in the collective dynamics of the catalytically important proline-binding loop. Overall, this study provides insights into the interplay of coupled dynamics and enzyme catalysis in prokaryotic-like ProRSs.

The two point mutations, G217A and E218A, were found to significantly impact proline activation, indicating that these noncatalytic residues are crucial for function. The mutation of G217 and E218 to alanine only mildly impacted cognate tRNA aminoacylation. This observation suggests that the binding of the 3′-acceptor end in the aminoacylation active site was not altered significantly by these mutations.

MD simulations of three point mutants (G217A, E218A, and E218D) and the deletion mutant (ΔINS) demonstrated that the overall fluctuations of the backbone were impacted differently among these enzymes. A reduction in backbone fluctuation was evident in the case of G217A and E218D, indicating more rigidity in the structure, while for E218A, a more flexible backbone was observed. For ΔINS, an overall reduction in flexibility was noted amidst a sharp increase in the number of fluctuations in the PBL.

The collective motion of PBL was studied by performing dynamic cross-correlation analyses (Figure 6), which demonstrated that the editing domain in the wild-type enzyme and the three mutants (G217A, E218A, and E218D) is quite flexible and engaged in anticorrelated motion with the activation domain. Although the basic coupling pattern did not change, the extents of correlations and anticorrelations were found to vary, consistent with the trend observed in the B factor analysis. In the case of G217A and E218D, the overall correlation among the structural elements surrounding the PBL is decreased, while for E218A, it is increased (Figure 5). This study indicates the role of E218 is not only to stabilize the substrate, as proposed previously,[14] but also to maintain PBL dynamics through coupled motion.

This study also provides insights into the severely reduced proline activation efficiency of ΔINS ProRS.[51] In the case of this variant, the analysis of the collective dynamics of the PBL revealed a total abolition of the coupling of motions with surrounding elements. Removal of the editing domain disrupts the hydrogen bonding network between polar residues at the domain−domain interface, which is important for the maintenance of the coupled protein dynamics (Figure 10) and optimal flexibility of protein segments surrounding the activation site. Although only the [217]GED[219] motif was targeted here, the role of other noncatalytic residues, such as N232 and E234, in the editing domain of Ec ProRS can be explored in the future.

Taken together, this work provides an understanding of how noncatalytic residues in a distant site modulate the activity of prokaryotic-like ProRSs by maintaining the coupled protein dynamics essential for catalysis. This study also reveals a novel role for a synthetase editing domain and may explain why truncated or defunct editing domains have been maintained in some aminoacyl-tRNA synthetases, despite the lack of catalytic activity.[51,52]

■ ASSOCIATED CONTENT

Ⓢ Supporting Information

Kinetic plots of pre- and post-transfer editing reaction and root-mean-square projections from essential dynamics analysis of WT and two mutants (G217A and E218A) of Ec ProRS. This material is available free of charge via the Internet at http://pubs.acs.org.

■ AUTHOR INFORMATION

Corresponding Author

*S.B.: phone, (715) 836-2278; fax, (715) 836-4979; e-mail, bhattas@uwec.edu. K.M.-F.: phone, (614) 292-2021; fax, (614) 688-5402; e-mail, musier@chemistry.ohio-state.edu. S.H.: phone, (715) 836-3850; fax, (715) 836-4979; e-mail, hatis@uwec.edu.

Notes

The authors declare no competing financial interest.

■ ABBREVIATIONS

Ec, *E. coli*; ED, essential dynamics; Ef, *En. faecalis*; MD, molecular dynamics; INS, insertion domain; PBL, proline-binding loop; PCA, principal component analysis; PDB, Protein Data Bank; ProRS, prolyl-tRNA synthetase; RMSD, root-mean-square deviation; RMSP, root-mean-square projection; WT, wild-type.

■ REFERENCES

(1) Beuning, P. J., and Musier-Forsyth, K. (2000) Hydrolytic editing by a class II aminoacyl-tRNA synthetase. *Proc. Natl. Acad. Sci. U.S.A.* 97, 8916–8920.

(2) Beuning, P. J., and Musier-Forsyth, K. (2001) Species-specific differences in amino acid editing by class II prolyl-tRNA synthetase. *J. Biol. Chem.* 276, 30779–30785.

(3) Ahel, I., Stathopoulos, C., Ambrogelly, A., Sauerwald, A., Toogood, H., Hartsch, T., and Soll, D. (2002) Cysteine activation is an inherent in vitro property of prolyl-tRNA synthetases. *J. Biol. Chem.* 277, 34743–34748.

(4) Mascarenhas, A., Martinis, S. A., An, S., Rosen, A. E., and Musier-Forsyth, K. (2009) *Protein Engineering*, Vol. 22, Springer-Verlag, New York.

(5) Stehlin, C., Burke, B., Yang, F., Liu, H., Shiba, K., and Musier-Forsyth, K. (1998) Species-specific differences in the operational RNA code for aminoacylation of tRNAPro. *Biochemistry* 37, 8605–8613.

(6) Cusack, S., Yaremchuk, A., Krikliviy, I., and Tukalo, M. (1998) tRNA(Pro) anticodon recognition by *Thermus thermophilus* prolyl-tRNA synthetase. *Structure* 6, 101–108.

(7) Wong, F. C., Beuning, P. J., Nagan, M., Shiba, K., and Musier-Forsyth, K. (2002) Functional role of the prokaryotic proline-tRNA synthetase insertion domain in amino acid editing. *Biochemistry* 41, 7108–7115.

(8) Wong, F. C., Beuning, P. J., Silvers, C., and Musier-Forsyth, K. (2003) An isolated class II aminoacyl-tRNA synthetase insertion domain is functional in amino acid editing. *J. Biol. Chem.* 278, 52857–52864.

(9) An, S., and Musier-Forsyth, K. (2004) Trans-editing of Cys-tRNAPro by *Haemophilus influenzae* YbaK protein. *J. Biol. Chem.* 279, 42359–42362.

(10) An, S., and Musier-Forsyth, K. (2005) Cys-tRNA(Pro) editing by *Haemophilus influenzae* YbaK via a novel synthetase·YbaK·tRNA ternary complex. *J. Biol. Chem.* 280, 34465–34472.

(11) Hati, S., Ziervogel, B., Sternjohn, J., Wong, F. C., Nagan, M. C., Rosen, A. E., Siliciano, P. G., Chihade, J. W., and Musier-Forsyth, K. (2006) Pre-transfer editing by class II prolyl-tRNA synthetase: Role of aminoacylation active site in "selective release" of noncognate amino acids. *J. Biol. Chem.* 281, 27862–27872.

(12) Weimer, K. M., Shane, B. L., Brunetto, M., Bhattacharyya, S., and Hati, S. (2009) Evolutionary basis for the coupled-domain motions in *Thermus thermophilus* leucyl-tRNA synthetase. *J. Biol. Chem.* 284, 10088–10099.

(13) Bu, Z., Biehl, R., Monkenbusch, M., Richter, D., and Callaway, D. J. (2005) Coupled protein domain motion in Taq polymerase revealed by neutron spin-echo spectroscopy. *Proc. Natl. Acad. Sci. U.S.A.* 102, 17646–17651.

(14) Crepin, T., Yaremchuk, A., Tukalo, M., and Cusack, S. (2006) Structures of two bacterial prolyl-tRNA synthetases with and without a cis-editing domain. *Structure* 14, 1511–1525.

(15) Burke, B., Lipman, R. S., Shiba, K., Musier-Forsyth, K., and Hou, Y. M. (2001) Divergent adaptation of tRNA recognition by *Methanococcus jannaschii* prolyl-tRNA synthetase. *J. Biol. Chem.* 276, 20286–20291.

(16) Stehlin, C., Heacock, D. H. II, Liu, H., and Musier-Forsyth, K. (1997) Chemical modification and site-directed mutagenesis of the single cysteine in motif 3 of class II *Escherichia coli* prolyl-tRNA synthetase. *Biochemistry* 36, 2932–2938.

(17) Fersht, A. R., Ashford, J. S., Bruton, C. J., Jakes, R., Koch, G. L., and Hartley, B. S. (1975) Active site titration and aminoacyl adenylate binding stoichiometry of aminoacyl-tRNA synthetases. *Biochemistry* 14, 1–4.

(18) Liu, H., and Musier-Forsyth, K. (1994) *Escherichia coli* proline tRNA synthetase is sensitive to changes in the core region of tRNA(Pro). *Biochemistry* 33, 12708–12714.

(19) Heacock, D., Forsyth, C. J., Shiba, K., and Musier-Forsyth, K. (1996) *Bioorg. Chem.* 24, 273–289.

(20) Musier-Forsyth, K., Scaringe, S., Usman, N., and Schimmel, P. (1991) Enzymatic aminoacylation of single-stranded RNA with an RNA cofactor. *Proc. Natl. Acad. Sci. U.S.A.* 88, 209–213.

(21) Humphrey, W., Dalke, A., and Schulten, K. (1996) VMD: Visual molecular dynamics. *J. Mol. Graphics* 14, 27–38.

(22) MacKerell, A. D. J., Bashford, D., Bellott, M., Dunbrack, R. L. J., Evanseck, J. D., Field, M. J., Fischer, S., Gao, J., Gou, J., Ha, S., Joseph-McCarthy, D., Kuchnir, L., Kuczera, K., Lau, F. T. K., Mattos, C., Michnick, S., Ngo, T., Nguyen, D. T., Prodhom, B., Reiher, W. E. I., Roux, B., Schelenkrich, M., Smith, J. C., Stote, R., Straub, J., Watanbe, M., Wiórkiewicz-Kuczera, J., Yin, D., and Karplus, M. (1998) All-atom empirical potential for molecular modeling and dynamics studies of proteins. *J. Phys. Chem. B* 102, 3586.

(23) Phillips, J. C., Braun, R., Wang, W., Gumbart, J., Tajkhorshid, E., Villa, E., Chipot, C., Skeel, R. D., Kale, L., and Schulten, K. (2005) Scalable molecular dynamics with NAMD. *J. Comput. Chem.* 26, 1781–1802.

(24) Jorgensen, W. L., Chandrasekhar, J., Madura, J. D., Impey, R. W., and Klein, M. L. (1983) Comparison of simple potential functions for simulating liquid water. *J. Chem. Phys.* 79, 926.

(25) Ryckaert, J. P., Ciotti, G., and Berensden, H. J. C. (1977) Numerical integration of the Cartesian equations of motion of a system with constraints: Molecular dynamics of n-alkanes. *J. Comput. Phys.* 23, 327–341.

(26) Darden, T., York, D., and Pedersen, L. (1993) Particle Mesh Ewald: An N.Log(N) Method for Ewald Sums in Large Systems. *J. Chem. Phys.* 98, 10089–10092.

(27) Berendsen, H. J. C., Postma, J. P., van Gunsteren, M. W. F., DiNola, A., and Haak, J. R. (1984) Molecular dynamics with coupling to an external bath. *J. Chem. Phys.* 81, 3684–3690.

(28) Feller, S. E., Zhang, Y., Pastor, R. W., and Brooks, B. R. (1995) Constant pressure molecular dynamics simulation: The Langevin piston method. *J. Chem. Phys.* 103, 4613–4621.

(29) Martyna, G. J., Tobias, D. J., and Klein, M. L. (1994) Constant pressure molecular dynamics algorithms. *J. Chem. Phys.* 101, 4177–4189.

(30) Bhattacharyya, S., Ma, S., Stankovich, M. T., Truhlar, D. G., and Gao, J. (2005) Potential of mean force calculation for the proton and hydride transfer reactions catalyzed by medium-chain acyl-CoA dehydrogenase: Effect of mutations on enzyme catalysis. *Biochemistry 44*, 16549−16562.

(31) Rauschnot, J. C., Yang, C., Yang, V., and Bhattacharyya, S. (2009) Theoretical determination of the redox potentials of NRH:quinone oxidoreductase 2 using quantum mechanical/molecular mechanical simulations. *J. Phys. Chem. B 113*, 8149−8157.

(32) Peters, G. H., van Aalten, D. M., Svendsen, A., and Bywater, R. (1997) Essential dynamics of lipase binding sites: The effect of inhibitors of different chain length. *Protein Eng. 10*, 149−158.

(33) van Aalten, D. M., Amadei, A., Linssen, A. B., Eijsink, V. G., Vriend, G., and Berendsen, H. J. (1995) The essential dynamics of thermolysin: Confirmation of the hinge-bending motion and comparison of simulations in vacuum and water. *Proteins 22*, 45−54.

(34) Mueller, R. M., North, M. A., Yang, C., Hati, S., and Bhattacharyya, S. (2011) Interplay of flavin's redox states and protein dynamics: An insight from QM/MM simulations of dihydronicotinamide riboside quinone oxidoreductase 2. *J. Phys. Chem. B 115*, 3632−3641.

(35) Glykos, N. M. (2006) Software news and updates. Carma: A molecular dynamics analysis program. *J. Comput. Chem. 27*, 1765−1768.

(36) Amadei, A., Linssen, A. B., and Berendsen, H. J. (1993) Essential dynamics of proteins. *Proteins 17*, 412−425.

(37) Kazmierkiewicz, R., Czaplewski, C. C., Lammek, B., and Ciarkowski, J. (1999) Essential Dynamics/Factor Analysis for the Interpretation of Molecular Dynamics Trajectories. *J. Comput.-Aided Mol. Des. 13*, 21−33.

(38) Jabukowski, H., and Goldman, E. (1992) Editing of errors in selection of amino acids for protein synthesis. *Microbiol. Rev. 56*, 412−429.

(39) Beuning, P. J., and Musier-Forsyth, K. (2001) Species-specific differences in amino acid editing by class II prolyl-tRNA synthetase. *J. Biol. Chem. 276*, 30779−30785.

(40) Yang, L. W., and Bahar, I. (2005) Coupling between catalytic site and collective dynamics: A requirement for mechanochemical activity of enzymes. *Structure 13*, 893−904.

(41) Tousignant, A., and Pelletier, J. N. (2004) Protein motions promote catalysis. *Chem. Biol. 11*, 1037−1042.

(42) Hammes-Schiffer, S., and Benkovic, S. J. (2006) Relating protein motion to catalysis. *Annu. Rev. Biochem. 75*, 519−541.

(43) Bakan, A., and Bahar, I. (2009) The intrinsic dynamics of enzymes plays a dominant role in determining the structural changes induced upon inhibitor binding. *Proc. Natl. Acad. Sci. U.S.A. 106*, 14349−14354.

(44) Agarwal, P. K. (2005) Role of protein dynamics in reaction rate enhancement by enzymes. *J. Am. Chem. Soc. 127*, 15248−15256.

(45) Agarwal, P. K., Billeter, S. R., Rajagopalan, P. T., Benkovic, S. J., and Hammes-Schiffer, S. (2002) Network of coupled promoting motions in enzyme catalysis. *Proc. Natl. Acad. Sci. U.S.A. 99*, 2794−2799.

(46) Eisenmesser, E. Z., Millet, O., Labeikovsky, W., Korzhnev, D. M., Wolf-Watz, M., Bosco, D. A., Skalicky, J. J., Kay, L. E., and Kern, D. (2005) Intrinsic dynamics of an enzyme underlies catalysis. *Nature 438*, 117−121.

(47) Henzler-Wildman, K. A., Lei, M., Thai, V., Kerns, S. J., Karplus, M., and Kern, D. (2007) A hierarchy of timescales in protein dynamics is linked to enzyme catalysis. *Nature 450*, 913−916.

(48) Rajagopalan, P. T., Lutz, S., and Benkovic, S. J. (2002) Coupling interactions of distal residues enhance dihydrofolate reductase catalysis: Mutational effects on hydride transfer rates. *Biochemistry 41*, 12618−12628.

(49) Tukalo, M., Yaremchuk, A., Fukunaga, R., Yokoyama, S., and Cusack, S. (2005) The crystal structure of leucyl-tRNA synthetase complexed with tRNALeu in the post-transfer-editing conformation. *Nat. Struct. Mol. Biol. 12*, 923−930.

(50) Silvian, L. F., Wang, J., and Steitz, T. A. (1999) Insights into editing from an ile-tRNA synthetase structure with tRNAile and mupirocin. *Science 285*, 1074−1077.

(51) SternJohn, J., Hati, S., Siliciano, P. G., and Musier-Forsyth, K. (2007) Restoring species-specific posttransfer editing activity to a synthetase with a defunct editing domain. *Proc. Natl. Acad. Sci. U.S.A. 104*, 2127−2132.

(52) Lue, S. W., and Kelley, S. O. (2005) An aminoacyl-tRNA synthetase with a defunct editing site. *Biochemistry 44*, 3010−3016.

■ NOTE ADDED AFTER ASAP PUBLICATION

This paper published ASAP on March 1, 2012. Minor typographical changes were made in the introduction and Results sections and the revised version was reposted on March 5, 2012.